ULTRA SONO GRAPHY

A prospective comparison of two ultrasound attenuation imaging modes using different frequencies for assessing hepatic steatosis

Hyeon Ji Jang[1], Jong Keon Jang[1], Subin Heo[1], Boyeon Koo[1], In Hye Song[2], Hee Jun Park[1], Seonghun Yoon[3], So Yeon Kim[1]

[1]Department of Radiology and Research Institute of Radiology, Asan Medical Center, University of Ulsan College of Medicine, Seoul; [2]Department of Pathology, Asan Medical Center, University of Ulsan College of Medicine, Seoul; [3]Asan Medical Center, University of Ulsan College of Medicine, Seoul, Korea

ORIGINAL ARTICLE

https://doi.org/10.14366/usg.24223
eISSN: 2288-5943
Ultrasonography 2025;44:202-211

Purpose: This study compared the diagnostic performance of two attenuation imaging (ATI) modes—low-frequency (3 MHz) and high-frequency (4 MHz)—for assessing hepatic steatosis, with histopathological hepatic fat fraction (HFF) as the reference standard.

Methods: This prospective single-center study enrolled participants with suspected metabolic dysfunction-associated steatotic liver disease (MASLD) scheduled for liver biopsy or surgery between June 2023 and June 2024. Attenuation coefficient (AC) values were consecutively measured using low- and high-frequency ATI modes, while the skin-to-region of interest distance (SRD) was measured simultaneously. Spearman correlation analysis evaluated the relationships of AC with HFF and SRD, and linear regression identified factors affecting AC. Diagnostic performance was evaluated using the area under the receiver operating characteristic curve (AUROC).

Results: In total, 119 participants (mean age, 37.2±12.0 years; 87 men) were included, with 73 (61.3%) diagnosed with MASLD. HFF ranged from 0% to 50%. The AC values in the low-frequency mode were significantly higher than those in the high-frequency mode (0.61 vs. 0.54 dB/cm/MHz, P<0.001). HFF significantly influenced AC in both modes, whereas SRD affected AC only in the high-frequency mode (P<0.001). AC correlated positively with HFF in both modes (r_s≥0.514, P<0.001) and negatively with SRD in the high-frequency mode (r_s=−0.338, P<0.001). The AUROC for hepatic steatosis did not differ significantly between the two modes (0.751 vs. 0.771, P=0.609).

Conclusion: The low-frequency mode produced higher AC values than the high-frequency mode and demonstrated comparable diagnostic accuracy for assessing hepatic steatosis. Unlike the high-frequency mode, the low-frequency mode was not influenced by SRD.

Keywords: Attenuation imaging; Attenuation coefficient; Metabolic dysfunction-associated steatotic liver disease

Key points: The low-frequency mode yielded a higher attenuation coefficient compared to the high-frequency mode, with values that correlated positively with histopathologic hepatic fat fraction and remained unaffected by skin-to-region of interest distance. Therefore, the low-frequency mode appears more appropriate for assessing hepatic steatosis in patients with metabolic dysfunction-associated steatotic liver disease, particularly those with thick subcutaneous fat.

Received: December 28, 2024
Revised: March 3, 2025
Accepted: March 6, 2025

Correspondence to:
Jong Keon Jang, MD, PhD, Department of Radiology and Research Institute of Radiology, Asan Medical Center, University of Ulsan College of Medicine, 88 Olympic-ro 43-gil, Songpa-gu, Seoul 05505, Korea
Tel. +82-2-3010-0332
Fax. +82-2-2045-4127
E-mail: jongkeon.jang@gmail.com

This is an Open Access article distributed under the terms of the Creative Commons Attribution Non-Commercial License (http://creativecommons.org/licenses/by-nc/4.0/) which permits unrestricted non-commercial use, distribution, and reproduction in any medium, provided the original work is properly cited.

Copyright © 2025 Korean Society of Ultrasound in Medicine (KSUM)

How to cite this article:
Jang HJ, Jang JK, Heo S, Koo B, Song IH, Park HJ, et al. A prospective comparison of two ultrasound attenuation imaging modes using different frequencies for assessing hepatic steatosis. Ultrasonography. 2025 May;44(3):202-211.

Introduction

Metabolic dysfunction-associated steatotic liver disease (MASLD), characterized by excessive hepatic fat accumulation, has emerged as a major global liver disease [1–3]. Hepatic steatosis is a central component of MASLD and, if left untreated, may progress to metabolic dysfunction-associated steatohepatitis, liver fibrosis, and eventually cirrhosis [4–6]. Effective management and treatment of MASLD critically depend on early detection and continuous monitoring of hepatic steatosis severity, which are essential for preventing disease progression. Although liver biopsy remains the gold standard for diagnosing and grading hepatic steatosis, its invasive nature and inter-observer variability limit its use for routine follow-up in clinical practice [7,8]. Although the magnetic resonance imaging (MRI) proton density fat fraction has emerged as a noninvasive alternative for evaluating hepatic steatosis [9–11], its widespread implementation is hindered by high costs and limited accessibility.

As a first-line diagnostic tool, ultrasonography is commonly used to detect hepatic steatosis in the general population. Among the various quantitative ultrasonography-based techniques, the controlled attenuation parameter (CAP) derived from transient elastography (TE) (Fibroscan, Echosens, Paris, France) has been widely employed in observational studies and clinical trials [9,12,13]. The introduction of the XL probe (2.5 MHz) for TE has enhanced the applicability of CAP in patients with MASLD by reducing failure rates associated with the conventional M probe (3.5 MHz), especially in obese individuals [14,15]. However, previous studies have reported discrepancies in CAP values between these probes, potentially affecting the assessment of hepatic steatosis [14,16]. Recently, the attenuation coefficient (AC), measured using attenuation imaging (ATI), has gained attention as a quantitative ultrasound method for assessing hepatic steatosis while simultaneously visualizing the liver with B-mode ultrasound [17–19]. Unlike TE, ATI provides the advantage of direct liver visualization and precise measurement of the target area. Similar to CAP measurement, ATI employs two different modes that use different ultrasound frequencies (3 MHz vs. 4 MHz) to evaluate hepatic steatosis. Nevertheless, the diagnostic performance of AC measurements using these two ATI modes—particularly in comparison with histopathology as the reference standard—has not been comprehensively investigated.

Therefore, this study aimed to evaluate and compare the diagnostic performance of the two ATI modes in assessing hepatic steatosis and to identify factors affecting AC values in each mode among participants with suspected MASLD.

Materials and Methods

Compliance with Ethical Standards

This prospective single-center study received approval from the institutional review board of Asan Medical Center (approval No. 2022-1426), and written informed consent was obtained from all participants. The study protocol was registered at ClinicalTrials.gov (NCT 05855239).

Study Participants

Given the exploratory nature of this pilot study examining the diagnostic performance of two ATI modes, no formal sample size calculation was performed, and the study continued until 120 participants were enrolled. The study consecutively enrolled participants scheduled for liver biopsy or surgery within seven days after undergoing ultrasonography at a single tertiary hospital between June 2023 and June 2024, either for liver donation or liver disease. The inclusion criteria were as follows: (1) age between 18 and 80 years, (2) body mass index (BMI) ≥23 kg/m^2, and (3) suspected hepatic steatosis on imaging examinations such as ultrasound, computed tomography, or MRI [3,20,21]. Participants were excluded if they had excessive alcohol consumption (exceeding 30 g/day for men and 20 g/day for women) [3], liver disease other than MASLD, a history of liver surgery, or a large or infiltrative mass in the right liver. Furthermore, participants scheduled for liver biopsy were excluded if they exhibited a tendency for excessive bleeding (platelets <50,000/μL, prothrombin time international normalized ratio >1.5) (Fig. 1). The clinical characteristics, anthropometric measurements, and laboratory findings of the participants were recorded.

Ultrasonography Examinations

Two abdominal radiologists (H.J.J. and J.K.J., with 5 and 8 years of abdominal ultrasound experience, respectively) independently evaluated all participants for hepatic steatosis using AC measurements obtained during ATI performed with an Aplio i800 ultrasound scanner (Canon Medical Systems, Otawara, Japan). For this study, AC was measured twice in each participant using two different ultrasound frequencies available in ATI: 3.0 MHz for the low-frequency mode and 4.0 MHz for the high-frequency mode, with a 1–8 MHz curvilinear transducer. To minimize potential bias from measurement order, the sequence of the two frequencies was alternated every two months. The examination was performed via a right intercostal approach while the patient maintained a breath-hold in the supine position. For both measurements, a fan-shaped sampling box (4×8 cm) displaying color-coded attenuation levels was positioned at consistent depths in the right anterior section of

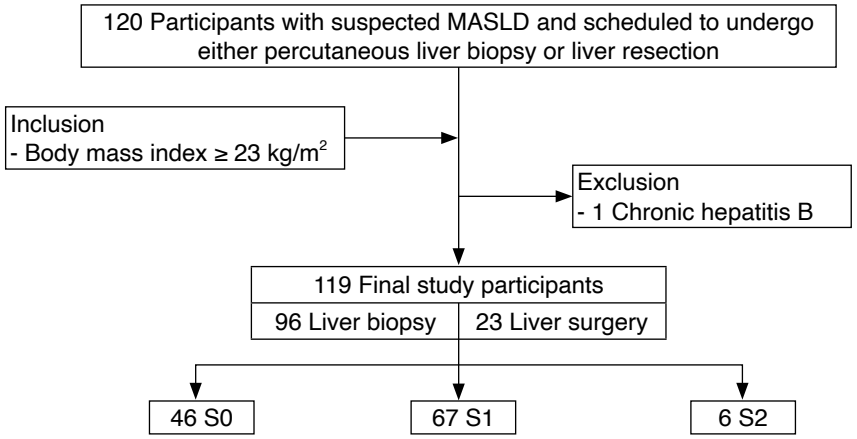

Fig. 1. Flow chart of patient enrollment. Steatosis was defined according to the percentage of affected hepatocytes: S0, <5%; S1, 5%–33%; S2, >33%–66%. MASLD, metabolic dysfunction-associated steatotic liver disease.

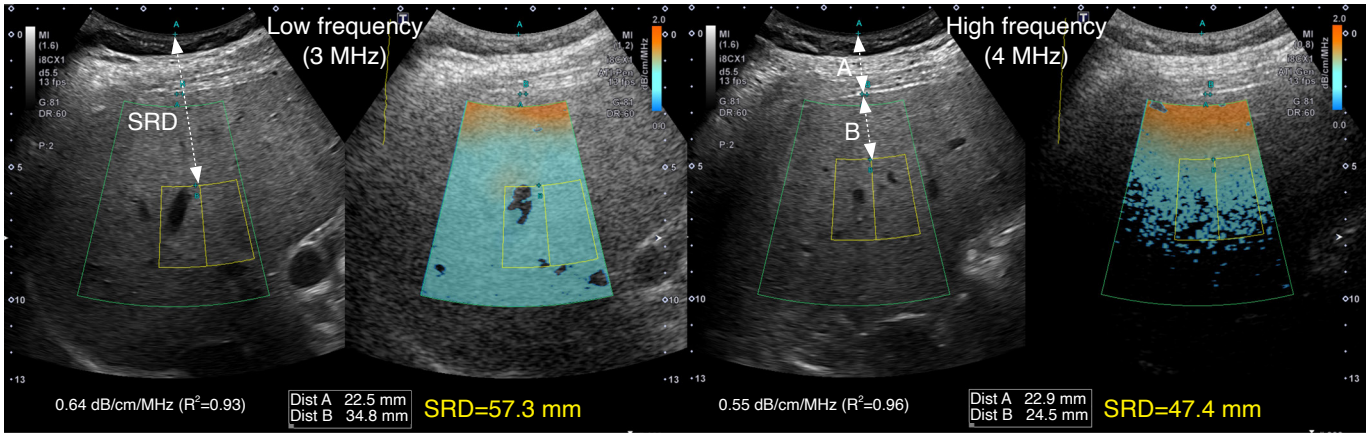

Fig. 2. Measurements of attenuation coefficient (AC) using low-frequency and high-frequency attenuation imaging modes in a 29-year-old man with metabolic dysfunction-associated steatotic liver disease. A represents the skin-to-capsule distance, while B indicates the distance from the liver capsule to the region of interest (ROI). The sum of these two distances represents the skin-to-ROI distance (SRD). Despite a greater SRD in the low-frequency mode (57.3 mm) than in the high-frequency mode (47.4 mm), the AC is higher in low-frequency mode (0.64 dB/cm/MHz) than in high-frequency mode (0.55 dB/cm/MHz). All measurements were valid (R^2>0.8). The patient underwent an ultrasonography-guided liver biopsy for liver donation, with a hepatic fat fraction of 25% being reported on pathology.

the liver (Fig. 2). A 2×4-cm region of interest (ROI) was placed in a nearly identical location across modes, specifically in areas with homogeneous color-coded attenuation within the mid to lower two-thirds of the sampling box. This approach was designed to avoid overestimation due to reverberation artifacts and underestimation from areas of high attenuation, as suggested by previous studies [22–24]. Additional technical details on AC measurements are available elsewhere [25,26]. Five AC values were obtained in each mode, yielding a total of 10 measurements per participant. AC values with R^2 ≥0.8 were considered valid, and measurements with an interquartile range (IQR)/median <30% were deemed reliable [26,27]. The median of the five measurements was used to represent the AC value for each mode, irrespective of validity or reliability. Measurements were also made of the skin-to-liver capsule distance (SCD) and the distance from the liver capsule to the ROI. The skin-to-ROI distance (SRD) was calculated as the sum of these two distances (Supplementary Fig. 1). For participants undergoing liver biopsy, an ultrasonography-guided percutaneous procedure was performed near the area where the AC value was measured.

Histopathologic Evaluation

Liver tissue samples obtained via biopsy or surgical resection were independently evaluated by an experienced pathologist under blinded conditions. Hepatic steatosis was visually quantified as the hepatic fat fraction (HFF), defined by the percentage of hepatocytes containing fat droplets on hematoxylin-eosin-stained specimens. Hepatic steatosis, hepatocyte ballooning, and lobular inflammatory activity were evaluated according to the nonalcoholic steatohepatitis clinical research scoring system, which grades steatosis (S0, <5%; S1, 5%–33%; S2, >33%–66%; S3, >66%), lobular inflammation

on a scale of 0 to 3, and ballooning degeneration on a scale of 0 to 2 [28]. Liver fibrosis was classified as F0 (no fibrosis), F1 (portal fibrosis without septa), F2 (portal fibrosis with few septa), F3 (bridging fibrosis without cirrhosis), or F4 (cirrhosis) according to the Meta-Analysis of Histological Data in Viral Hepatitis scoring system [29].

Statistical Analysis

The feasibility of the two ATI modes was assessed by comparing the proportions of valid measurements (defined as the number of measurements with $R^2 \geq 0.8$ out of five per mode) and reliable measurements (IQR/median<30%) using the McNemar test. Agreement in AC and SRD values between the two ATI modes was evaluated using Bland-Altman plots. The correlation of AC with HFF and SRD was analyzed using scatter plots and Spearman's correlation analysis. Factors associated with AC were identified using linear regression analysis on logarithmically transformed AC values. Variables with a P-value <0.1 in the univariable analysis were entered into multivariable linear regression. The diagnostic performance of AC for hepatic steatosis (S≥1) was assessed using receiver operating characteristic (ROC) curves, and the areas under the ROC curves for both ATI modes were compared using the DeLong method. For both ATI modes, cutoff values for ruling out and ruling in S≥1 were established by selecting thresholds with sensitivities above 90% and specificities above 90%, respectively. Statistical significance was defined as a P<0.05. All statistical analyses were performed using SPSS version 21 (IBM Corp., Armonk, NY, USA) and MedCalc software version 22.032 (Ostend, Belgium).

Results

Participant Characteristics

Of the 120 consecutive participants enrolled during the study period, 119 Asian participants (mean age, 37.2±12 years; 87 men) were finally included in this study, after excluding one participant who tested positive for hepatitis B surface antigen (Fig. 1). Among the 119 participants, 106 (89.1%) were candidates for liver donation, 12 (10.1%) underwent liver surgery for a hepatic mass, and one (0.8%) underwent liver biopsy for liver cirrhosis. The characteristics of the study population are summarized in Table 1. The mean BMI was 27.7 kg/m^2 (standard deviation [SD], 3.2), with 101 participants (84.9%) having a BMI≥25 kg/m^2 and 21 participants (17.6%) having a BMI≥30 kg/m^2. Histopathologic assessment was performed via percutaneous liver biopsy in 96 participants (80.7%) and surgical resection in 23 participants (19.3%). The interval between ultrasonography and tissue acquisition ranged from 0 to 4 days, with a median of 0 days. Histopathologic HFF ranged from 0% to

Table 1. Characteristics of the 119 participants

Characteristic	Value
Age (year)	37.2±12.0
Male sex	87 (73.1)
BMI (kg/m^2)	27.7±3.2
≥25	101 (84.9)
≥30	21 (17.6)
Laboratory finding	
AST (IU/L)	21 (18–25.5)
ALT (IU/L)	19 (14–26)
Total bilirubin (mg/dL)	0.6 (0.4–0.7)
Glucose (mg/dL)	96 (91–103)
Total cholesterol (mg/dL)	174 (151.5–205)
Triglycerides (mg/dL)	122.5 (82.8–183.3)
HDL-cholesterol (mg/dL)	46 (40–54)
Albumin (g/dL)	4.3 (4.1–4.5)
Histopathologic finding	
Hepatic fat fraction (%)	8.8±9.4
Steatosis grade	
S0 (<5%)	46 (38.7)
S1 (5%–33%)	67 (56.3)
S2 (>33%–66%)	6 (5.0)
Hepatocyte ballooning grade	
B0	89 (74.8)
B1	26 (21.8)
B2	4 (3.4)
Lobular inflammation grade	
I0	80 (67.2)
I1	33 (27.7)
I2	6 (5.0)
I3	0
Fibrosis grade	
F0	106 (89.1)
F1	3 (2.5)
F2	4 (3.4)
F3	4 (3.4)
F4	2 (1.7)
Diagnosis	
Liver with less than 5% fat fraction	46 (38.7)
MASL	26 (21.8)
MASH	47 (39.5)

Values are presented as mean±standard deviation, number (%), or median (IQR).
BMI, body mass index; AST, aspartate aminotransferase; ALT, alanine aminotransferase; HDL, high-density lipoprotein; MASL, metabolic dysfunction-associated steatotic liver; MASH, metabolic dysfunction-associated steatohepatitis; IQR, interquartile range.

50%, with a mean of 8.8% (SD, 9.4). Forty-six participants (38.7%) were diagnosed with an HFF of less than 5%, whereas 73 (61.3%) were diagnosed with MASLD (26 without steatohepatitis and 47 with steatohepatitis).

Measurement of AC

The mean SRD for AC measurement differed slightly between the two ATI modes, though the difference was statistically significant (low-frequency 42.7 mm vs. high-frequency 41.5 mm; 95% limits of agreement, 1.2798±7.0084 mm; P<0.001) (Table 2, Fig. 3). Similarly, the mean distance from the liver capsule to the ROI differed minimally between the two ATI modes (low-frequency 22.9 mm vs. high-frequency 21.5 mm, P<0.001). The median AC values were 0.61 dB/cm/MHz (IQR, 0.56 to 0.67) for the low-frequency mode and 0.54 dB/cm/MHz (IQR, 0.50 to 0.60) for the high-frequency mode. Despite the deeper ROI in the low-frequency mode, AC was significantly higher in the low-frequency mode than in the high-frequency mode (95% limits of agreement, 0.0593±0.1307 dB/cm/MHz; P<0.001) (Fig. 3). In the low-frequency mode, all measured AC values were valid (R^2≥0.8) and reliable (IQR/median<30%), whereas in the high-frequency mode, 98.3% of AC values were valid and 100% were reliable; there was no significant difference between the two modes (P>0.5). ACs in both modes positively correlated with histopathologic HFF (low-frequency: r_s=0.514; 95% confidence interval [CI], 0.368 to 0.635; high-frequency: r_s=0.614; 95% CI, 0.487 to 0.715; both P<0.001). There was a significant negative correlation between AC and SRD in the high-frequency mode (r_s=−0.338; 95% CI, −0.488 to −0.168; P<0.001) (Fig. 4).

Factors Affecting the AC

Tables 3 and 4 summarize the associations between clinical and ultrasonography variables and AC values in the two ATI modes. In the low-frequency mode, histopathologic HFF, lobular inflammation, and hepatocyte ballooning were significant factors in the univariable

Table 2. Ultrasound parameters measured by the two different modes of attenuation imaging

	Low-frequency mode (3.0 MHz)	High-frequency mode (4.0 MHz)	P-value
Skin-to-liver capsule distance (mm)	19.1 (17.6–21.8)	19.7 (17.6–21.7)	0.450
Skin-to-ROI distance (mm)	42.7±6.2	41.5±4.9	<0.001
Liver capsule to ROI (mm)	22.9±5.1	21.5±4.2	<0.001
Attenuation coefficient (dB/cm/MHz)	0.61 (0.56–0.67)	0.54 (0.50–0.60)	<0.001
R^2≥0.8	119 (100)	117 (98.3)	0.500
IQR/median (%) <30	119 (100)	119 (100)	

Values are presented as median (IQR), mean±standard deviation, or number (%).
The R^2 values indicate the validity of the measurement and were categorized into poor (R^2<0.80), good (R^2=0.80–0.90), and excellent (R^2>0.90).
ROI, region of interest; IQR, interquartile range.

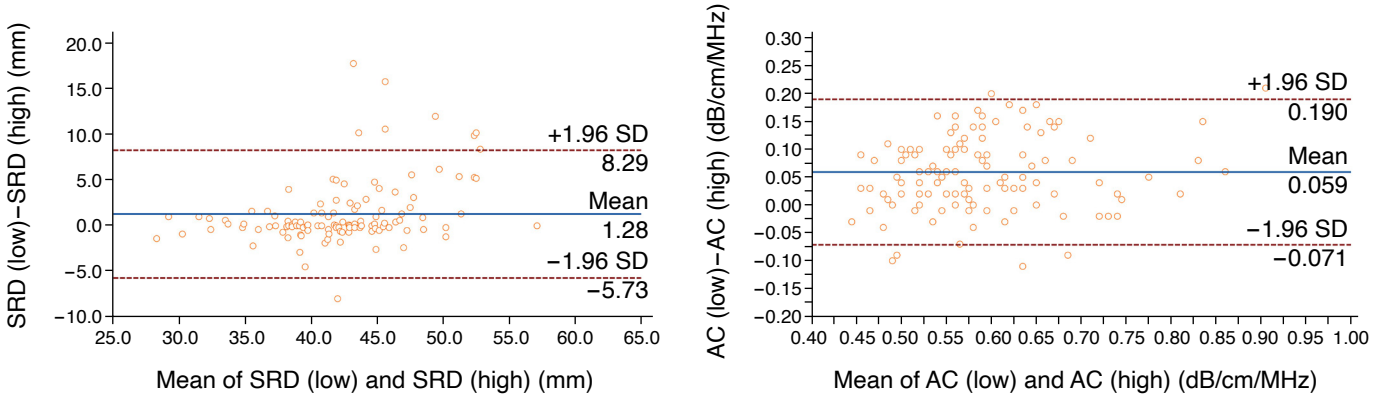

Fig. 3. Bland-Altman plots of skin to region of interest distance and attenuation coefficient in low-frequency (low) and high-frequency (high) attenuation imaging modes.
Bland-Altman plot of skin to region of interest distance (SRD) (low) and SRD (high) (A) and Bland-Altman plot of attenuation coefficient (AC) (low) and AC (high) (B) are shown. The solid blue lines represent the mean difference in SRD and AC values, respectively. The dashed lines define the 95% limits of agreement. SD, standard deviation.

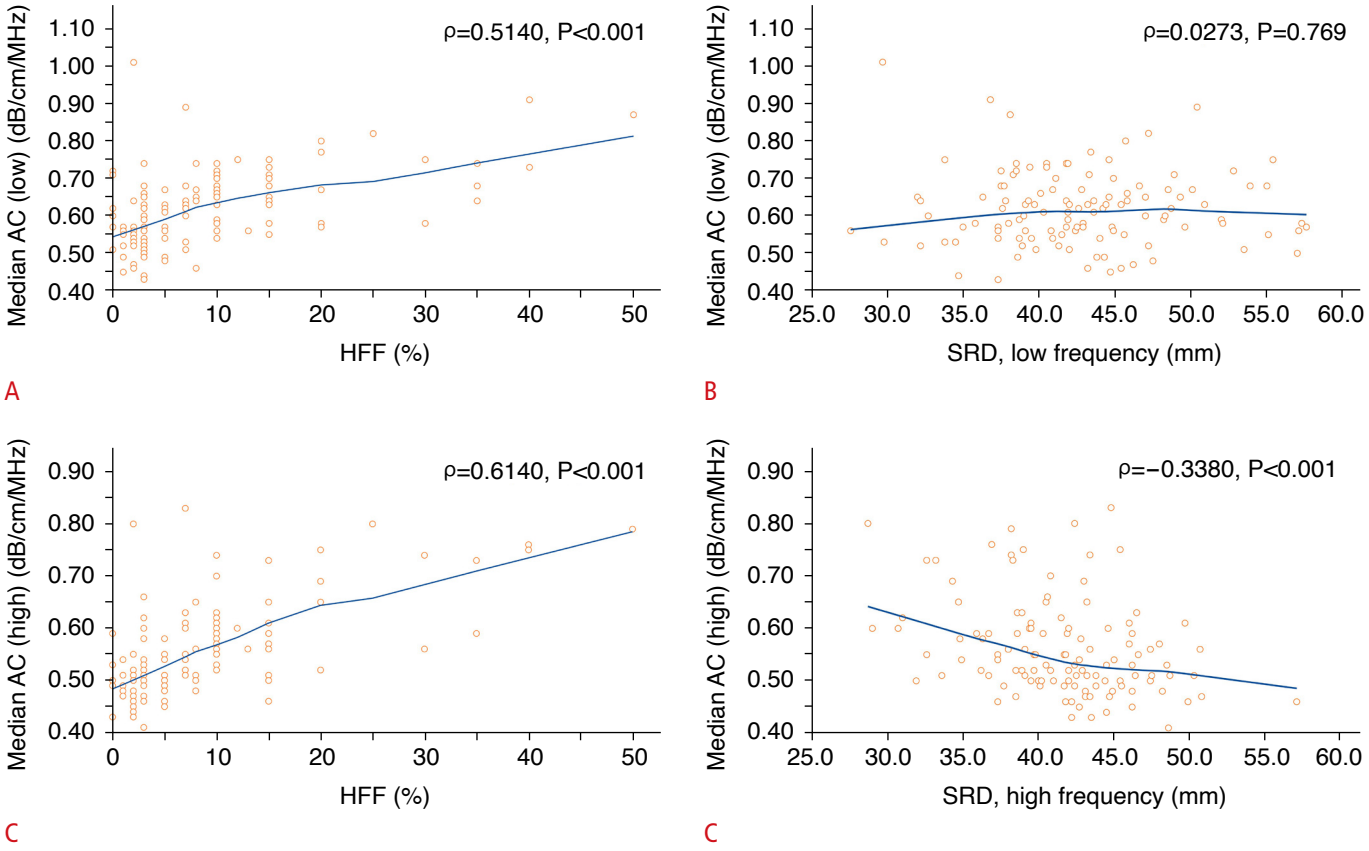

Fig. 4. Scatter plots of attenuation coefficient (AC) values in respect to hepatic fat fraction (HFF) (A, C) and skin to region of interest distance (SRD) (B, D) in low-frequency (low) and high-frequency (high) attenuation imaging modes.

Table 3. Factors affecting attenuation coefficients in the low-frequency mode

Factor	Univariable analysis			Multivariable analysis		
	Coefficient	95% CI	P-value	Coefficient	95% CI	P-value
Age	0.0005	−0.0001 to 0.0019	0.082	0.0004	−0.0006 to 0.0014	0.403
Sex	0.0054	−0.0222 to 0.0331	0.700	–	–	–
BMI	0.0023	−0.0016 to 0.0061	0.241	–	–	–
AST	0.0002	−0.0011 to 0.0015	0.760	–	–	–
ALT	−0.0003	−0.0008 to 0.0003	0.327	–	–	–
Glucose	0.0004	−0.0002 to 0.0011	0.189	–	–	–
Cholesterol/HDL	0.0005	−0.0093 to 0.0105	0.909	–	–	–
Triglyceride/HDL	0.0019	−0.0016 to 0.0054	0.283	–	–	–
Skin-to-capsule distance	0.0020	−0.0014 to 0.0065	0.212	–	–	–
Skin-to-ROI distance	−0.0001	−0.0021 to 0.0019	0.891	–	–	–
Hepatic fat fraction	0.0036	0.0024 to 0.0047	<0.001	0.0029	0.0015 to 0.0044	<0.001
Lobular inflammation	0.0417	0.0219 to 0.0614	<0.001	0.0115	−0.0117 to 0.0346	0.329
Hepatocyte ballooning	0.0385	0.0160 to 0.0610	0.001	0.0081	−0.0154 to 0.0315	0.496
Fibrosis	0.0113	−0.0036 to 0.0262	0.137	–	–	–

CI, confidence interval; BMI, body mass index; AST, aspartate aminotransferase; ALT, alanine aminotransferase; HDL, high-density lipoprotein cholesterol; ROI, region of interest.

Table 4. Factors affecting attenuation coefficients in the high-frequency mode

Factor	Univariable analysis			Multivariable analysis		
	Coefficient	95% CI	P-value	Coefficient	95% CI	P-value
Age	0.0007	−0.0003 to 0.0017	0.199	–	–	–
Sex	−0.0113	−0.0386 to 0.0159	0.412	–	–	–
BMI	0.0005	−0.0032 to 0.0044	0.770	–	–	–
AST	0.0007	−0.0006 to 0.0020	0.286	–	–	–
ALT	0.0001	−0.0004 to 0.0006	0.664	–	–	–
Glucose	0.0003	−0.0005 to 0.0009	0.540	–	–	–
Cholesterol/HDL	0.0048	−0.0050 to 0.0146	0.336	–	–	–
Triglyceride/HDL	0.0022	−0.0013 to 0.0056	0.214	–	–	–
Skin-to-capsule distance	−0.0027	−0.0066 to 0.0011	0.164	–	–	–
Skin-to-ROI distance	−0.0046	−0.0070 to −0.0023	<0.001	−0.0044	−0.0062 to −0.0025	<0.001
Hepatic fat fraction	0.0043	0.0033 to 0.0053	<0.001	0.0037	0.0025 to 0.0049	<0.001
Lobular inflammation	0.0418	0.0224 to 0.0613	<0.001	0.0146	−0.0038 to 0.0330	0.119
Hepatocyte ballooning	0.0325	0.0100 to 0.0550	0.005	0.0100	−0.0201 to 0.0190	0.955
Fibrosis	0.0123	−0.0024 to 0.0270	0.101	–	–	–

CI, confidence interval; BMI, body mass index; AST, aspartate aminotransferase; ALT, alanine aminotransferase; HDL, high-density lipoprotein cholesterol; ROI, region of interest.

analysis (P≤0.001). However, in the multivariable analysis, HFF was the only factor significantly associated with AC (P<0.001). In the high-frequency mode, SRD, HFF, lobular inflammation, and hepatocyte ballooning were significant in the univariable analysis (P≤0.005), while both SRD and HFF remained significantly associated with AC in the multivariable analysis (P<0.001).

Diagnostic Performance of AC for Hepatic Steatosis

For the diagnosis of steatosis (S≥1), the areas under the ROC curves for AC were 0.751 (95% CI, 0.636 to 0.826) for the low-frequency mode and 0.771 (95% CI, 0.685 to 0.843) for the high-frequency mode, with no statistically significant difference (P=0.609) (Supplementary Fig. 2). In the low-frequency mode, cutoff values of 0.54 and 0.68 dB/cm/MHz provided sensitivities above 90% for ruling out and specificities above 90% for ruling in S≥1. In the high-frequency mode, cutoff values of 0.49 and 0.60 dB/cm/MHz provided sensitivities and specificities greater than 90% for ruling out and ruling in, respectively, S≥1.

Discussion

In this study, hepatic steatosis was assessed by measuring the AC using two modes of ATI with different ultrasound frequencies (i.e., low-frequency and high-frequency modes). Both modes produced valid and reliable AC values, with comparable diagnostic accuracy for detecting hepatic steatosis. However, significant differences in actual AC values were observed between the two modes. AC values were significantly higher in the low-frequency mode compared to the high-frequency mode (0.61 dB/cm/MHz vs. 0.54 dB/cm/MHz, P<0.001). Histopathologic HFF was the only factor significantly associated with AC in the low-frequency mode, whereas both HFF and SRD were associated with AC in the high-frequency mode; notably, SRD showed a negative correlation with AC values.

The introduction of the XL probe (2.5 MHz) in CAP successfully reduced measurement failure rates and improved steatosis assessment in obese patients (BMI ≥30 kg/m² or SCD ≥25 mm), who frequently present with MASLD. Previous studies have shown that the XL probe yields significantly higher CAP values than the M probe (3.5 MHz) [14,16]. Similarly, in this study, the AC value obtained with the low-frequency mode (3.0 MHz) of ATI was significantly higher than that obtained with the high-frequency mode (4.0 MHz), consistent with previous findings using MRI-proton density fat fraction as a reference [30]. Unlike CAP in TE, ATI incorporates B-mode ultrasonography, allowing for precise ROI placement during AC measurement and thereby enhancing the evaluation of hepatic steatosis. Due to its greater penetration capability, the low-frequency mode targets slightly deeper liver regions, resulting in the sampling box being positioned farther from the ultrasound probe. Notably, even at this greater depth, the low-frequency mode still yielded higher AC values than the high-frequency mode.

AC has emerged as a promising tool for the identification and quantification of hepatic steatosis due to its noninvasiveness and cost-effectiveness [31,32]. Its application in ATI permits repeated measurements, facilitating longitudinal follow-up of patients with

hepatic steatosis. However, consistency in the ATI frequency is essential for accurate assessment of hepatic steatosis over time. Differences in SRD and AC values across various frequencies can introduce variability in the results. Moreover, the cutoff values for ruling in and ruling out hepatic steatosis vary between frequencies, with the low-frequency mode requiring a higher cutoff value for S1 than the high-frequency mode. Therefore, it is essential to use the same frequency during each assessment to ensure consistent and reliable quantification of hepatic steatosis.

HFF was significantly and positively correlated with AC in both low and high-frequency modes ($r_s \geq 0.514$, $P<0.001$). Conversely, SRD exhibited a negative correlation with AC in the high-frequency mode, while no such association was observed in the low-frequency mode. This distinction is particularly relevant for patients with MASLD, who are often obese and likely have a thick subcutaneous layer. Ultrasound attenuation at higher frequencies decreases more rapidly as it propagates through thick subcutaneous tissue; therefore, the low-frequency mode may be more suitable for these patients. Furthermore, CAP measurements are often not feasible for patients with cirrhosis from various etiologies, particularly when ascites is present, making ATI a valuable alternative. For such patients, the low-frequency mode may offer a significant advantage due to its ability to accommodate longer SRDs.

This study has several limitations. First, the proportion of obese participants (BMI ≥30 kg/m^2) was relatively small (17.6%), and the subcutaneous fat thickness over the liver was not substantial (median SCD, 19.1 to 19.6 mm). This may have contributed to the similar ROC curves for diagnosing hepatic steatosis, as well as the comparable validity and reliability observed between the two ATI modes. Consequently, it was not possible to propose cutoff values for SRD and BMI similar to those established for CAP (M vs. XL probe) in obese patients. To address these issues, future studies should include a cohort with a larger proportion of obese participants. Since only participants with BMI ≥23 kg/m^2 were included, the study results may not be generalizable to all suspected MASLD patients. Second, the participants predominantly represented the lower end of the MASLD spectrum, with only six (5.0%) having grade S2, 47 (39.5%) having metabolic dysfunction-associated steatohepatitis, and just two (1.7%) having cirrhosis. Therefore, it was not possible to compare the diagnostic accuracy of the two modes in patients with moderate hepatic steatosis (S≥2). The limited number of participants with advanced liver disease may have led to an underestimation of the impact of hepatic inflammation and fibrosis on AC measurements. Future research should include a broader range of MASLD severity. Third, there is a possibility of bias in the placement of the ROI box in each ATI mode. The SRD for AC measurement tended to be slightly greater (by 1.4 mm) in the low-frequency mode compared to the high-frequency mode. However, this difference was unavoidable in order to ensure valid AC measurements ($R^2 \geq 0.8$) within a uniform color-coded attenuation map. Additionally, this 1.4 mm difference in SRD may fall within the range of measurement error. Moreover, given that the AC values were significantly higher despite the deeper position in the low-frequency mode, this difference is considered meaningful. Fourth, AC was measured using an ultrasound platform from a single manufacturer. As a result, the findings of this study may not be generalizable to other attenuation-based ultrasound quantitative methods that employ different ultrasound frequency ranges or alternative methods for estimating the attenuation coefficient. Further studies should investigate whether these results are consistent across different platforms.

In conclusion, compared with the high-frequency mode, the low-frequency mode yielded higher AC values. AC measurements in the low-frequency mode were robust to changes in SRD, whereas those in the high-frequency mode showed a negative correlation with this distance. Given these findings, the low-frequency mode appears more appropriate for assessing hepatic steatosis in patients with metabolic dysfunction-associated steatotic liver disease, particularly those with thick subcutaneous fat.

ORCID: Hyeon Ji Jang: http://orcid.org/0000-0002-0858-6101; Jong Keon Jang: http://orcid.org/0000-0002-2938-6635; Subin Heo: http://orcid.org/0000-0002-4700-1014; Boyeon Koo: http://orcid.org/0009-0003-4073-5271; In Hye Song: http://orcid.org/0000-0001-6325-3548; Hee Jun Park: http://orcid.org/0009-0009-7666-5029; Seonghun Yoon: http://orcid.org/0009-0009-9362-3082; So Yeon Kim: https://orcid.org/0000-0001-6853-8577

Conflict of Interest

No potential conflict of interest relevant to this article was reported.

Acknowledgments

This work was granted by Canon Medical Systems Corporation and personal fees and financial supports (No. 2023-CMSK-UL002).

Supplementary Material

Supplementary Fig. 1. Measurement of skin-to-region of interest distance (SRD) in a 39-year-old woman with biopsy-proven metabolic dysfunction-associated steatohepatitis with steatosis grade S1 (https://doi.org/10.14366/usg.24223).

Supplementary Fig. 2. Receiver operating characteristics curves for attenuation coefficient (AC) values in low frequency and high frequency modes for steatosis grades of S0 versus S1 to S3, as defined by a hepatic fat fraction greater than 5% (https://doi.org/10.14366/usg.24223).

References

1. Hashimoto E, Taniai M, Tokushige K. Characteristics and diagnosis of NAFLD/NASH. J Gastroenterol Hepatol 2013;28 Suppl 4:64-70.
2. Younossi Z, Anstee QM, Marietti M, Hardy T, Henry L, Eslam M, et al. Global burden of NAFLD and NASH: trends, predictions, risk factors and prevention. Nat Rev Gastroenterol Hepatol 2018;15:11-20.
3. Kanwal F, Neuschwander-Tetri BA, Loomba R, Rinella ME. Metabolic dysfunction–associated steatotic liver disease: update and impact of new nomenclature on the American Association for the Study of Liver Diseases practice guidance on nonalcoholic fatty liver disease. Hepatology 2024;79:1212-1219.
4. Singh S, Allen AM, Wang Z, Prokop LJ, Murad MH, Loomba R. Fibrosis progression in nonalcoholic fatty liver vs nonalcoholic steatohepatitis: a systematic review and meta-analysis of paired-biopsy studies. Clin Gastroenterol Hepatol 2015;13:643-654.
5. McPherson S, Hardy T, Henderson E, Burt AD, Day CP, Anstee QM. Evidence of NAFLD progression from steatosis to fibrosing-steatohepatitis using paired biopsies: implications for prognosis and clinical management. J Hepatol 2015;62:1148-1155.
6. Hagstrom H, Shang Y, Hegmar H, Nasr P. Natural history and progression of metabolic dysfunction-associated steatotic liver disease. Lancet Gastroenterol Hepatol 2024;9:944-956.
7. Rockey DC, Caldwell SH, Goodman ZD, Nelson RC, Smith AD; American Association for the Study of Liver Diseases. Liver biopsy. Hepatology 2009;49:1017-1044.
8. Ratziu V, Charlotte F, Heurtier A, Gombert S, Giral P, Bruckert E, et al. Sampling variability of liver biopsy in nonalcoholic fatty liver disease. Gastroenterology 2005;128:1898-1906.
9. Caussy C, Alquiraish MH, Nguyen P, Hernandez C, Cepin S, Fortney LE, et al. Optimal threshold of controlled attenuation parameter with MRI-PDFF as the gold standard for the detection of hepatic steatosis. Hepatology 2018;67:1348-1359.
10. Caussy C, Reeder SB, Sirlin CB, Loomba R. Noninvasive, quantitative assessment of liver fat by MRI-PDFF as an endpoint in NASH trials. Hepatology 2018;68:763-772.
11. Loomba R, Sirlin CB, Ang B, Bettencourt R, Jain R, Salotti J, et al. Ezetimibe for the treatment of nonalcoholic steatohepatitis: assessment by novel magnetic resonance imaging and magnetic resonance elastography in a randomized trial (MOZART trial). Hepatology 2015;61:1239-1250.
12. Abeysekera KW, Fernandes GS, Hammerton G, Portal AJ, Gordon FH, Heron J, et al. Prevalence of steatosis and fibrosis in young adults in the UK: a population-based study. Lancet Gastroenterol Hepatol 2020;5:295-305.
13. Thiele M, Rausch V, Fluhr G, Kjaergaard M, Piecha F, Mueller J, et al. Controlled attenuation parameter and alcoholic hepatic steatosis: diagnostic accuracy and role of alcohol detoxification. J Hepatol 2018;68:1025-1032.
14. Caussy C, Brissot J, Singh S, Bassirian S, Hernandez C, Bettencourt R, et al. Prospective, same-day, direct comparison of controlled attenuation parameter with the M vs the XL probe in patients with nonalcoholic fatty liver disease, using magnetic resonance imaging-proton density fat fraction as the standard. Clin Gastroenterol Hepatol 2020;18:1842-1850.
15. de Ledinghen V, Hiriart JB, Vergniol J, Merrouche W, Bedossa P, Paradis V. Controlled attenuation parameter (CAP) with the XL probe of the Fibroscan((R)): a comparative study with the M probe and liver biopsy. Dig Dis Sci 2017;62:2569-2577.
16. Chan WK, Nik Mustapha NR, Mahadeva S, Wong VW, Cheng JY, Wong GL. Can the same controlled attenuation parameter cut-offs be used for M and XL probes for diagnosing hepatic steatosis? J Gastroenterol Hepatol 2018;33:1787-1794.
17. Fetzer DT, Rosado-Mendez IM, Wang M, Robbin ML, Ozturk A, Wear KA, et al. Pulse-echo quantitative US biomarkers for liver steatosis: toward technical standardization. Radiology 2022;305:265-276.
18. Park J, Lee JM, Lee G, Jeon SK, Joo I. Quantitative evaluation of hepatic steatosis using advanced imaging techniques: focusing on new quantitative ultrasound techniques. Korean J Radiol 2022;23:13-29.
19. Jang JK, Lee ES, Seo JW, Kim YR, Kim SY, Cho YY, et al. Two-dimensional shear-wave elastography and US attenuation imaging for nonalcoholic steatohepatitis diagnosis: a cross-sectional, multicenter study. Radiology 2022;305:118-126.
20. Hamer OW, Aguirre DA, Casola G, Lavine JE, Woenckhaus M, Sirlin CB. Fatty liver: imaging patterns and pitfalls. Radiographics 2006;26:1637-1653.
21. Starekova J, Hernando D, Pickhardt PJ, Reeder SB. Quantification of liver fat content with CT and MRI: state of the art. Radiology 2021;301:250-262.
22. Sugimoto K, Abe M, Oshiro H, Takahashi H, Kakegawa T, Tomita Y, et al. The most appropriate region-of-interest position for attenuation coefficient measurement in the evaluation of liver steatosis. J Med Ultrason (2001) 2021;48:615-621.
23. Ferraioli G, Filice C, Castera L, Choi BI, Sporea I, Wilson SR, et al. WFUMB guidelines and recommendations for clinical use of ultrasound elastography: Part 3: liver. Ultrasound Med Biol 2015;41:1161-1179.
24. Dietrich CF, Bamber J, Berzigotti A, Bota S, Cantisani V, Castera L, et al. EFSUMB guidelines and recommendations on the clinical use of liver ultrasound elastography, update 2017 (long version). Ultraschall Med 2017;38:e16-e47.
25. Tada T, Iijima H, Kobayashi N, Yoshida M, Nishimura T, Kumada T, et al. Usefulness of attenuation imaging with an ultrasound scanner for the evaluation of hepatic steatosis. Ultrasound Med Biol 2019;45:2679-2687.
26. Jeon SK, Lee JM, Joo I, Yoon JH, Lee DH, Lee JY, et al. Prospective

evaluation of hepatic steatosis using ultrasound attenuation imaging in patients with chronic liver disease with magnetic resonance imaging proton density fat fraction as the reference standard. Ultrasound Med Biol 2019;45:1407-1416.
27. Sugimoto K, Moriyasu F, Oshiro H, Takeuchi H, Abe M, Yoshimasu Y, et al. The role of multiparametric US of the liver for the evaluation of nonalcoholic steatohepatitis. Radiology 2020;296:532-540.
28. Kleiner DE, Brunt EM, Van Natta M, Behling C, Contos MJ, Cummings OW, et al. Design and validation of a histological scoring system for nonalcoholic fatty liver disease. Hepatology 2005;41:1313-1321.
29. Goodman ZD. Grading and staging systems for inflammation and fibrosis in chronic liver diseases. J Hepatol 2007;47:598-607.
30. Ferraioli G, Maiocchi L, Savietto G, Tinelli C, Nichetti M, Rondanelli M, et al. Performance of the attenuation imaging technology in the detection of liver steatosis. J Ultrasound Med 2021;40:1325-1332.
31. Jang JK, Choi SH, Lee JS, Kim SY, Lee SS, Kim KW. Accuracy of the ultrasound attenuation coefficient for the evaluation of hepatic steatosis: a systematic review and meta-analysis of prospective studies. Ultrasonography 2022;41:83-92.
32. Ferraioli G, Kumar V, Ozturk A, Nam K, de Korte CL, Barr RG. US attenuation for liver fat quantification: an AIUM-RSNA QIBA pulse-echo quantitative ultrasound initiative. Radiology 2022;302:495-506.